injected into a single site. Hence, each transcript preparation, with different RNA/lipofectin ratios, was injected at three separate sites. The chimpanzees were caged and maintained under conditions that met all relevant requirements for the use of primates in an approved facility. Animal protocols were reviewed and approved by the animal care and use committees from each institution involved with the chimpanzee studies. The chimpanzee experiments were also reviewed and approved by the Public Health Service Interagency Animal Model Committee.

17. Antibodies to HCV were measured by commercial enzyme immunoassays. The Abbott HCV EIA 2.0 assay (Abbott Laboratories, Abbot Park, IL) contains three recombinant HCV antigens: HC34, polyprotein amino acid residues 1 to 150 (HCV core protein); HC-31, residues 1192 to 1457 (an internal portion of NS3) and residues 1676 to 1931 (COOH-terminus of NS4A and most of NS4B); and c100-3, residues 1569 to 1931 (the COOH-terminal portion of NS3, NS4A, and most of NS4B). Antigen-specific reactivity of EIA-positive sera was further defined with the strip immunoblot assay RIBA HCV 2.0 SIA (Chiron Corporation, Emeryville, CA), which contains four recombinant antigens: c22-3, residues 2 to 120 (HCV core protein); c33c, residues 1192 to 1457 (internal region of NS3); c100-3; and 5-1-1, residues 1694 to 1735 (COOH-terminal portion of NS4A and NH_2-terminal portion of NS4B). Tests were performed according to the manufacturer's directions.
18. H. Popper, J. L. Dienstag, S. M. Feinstone, H. J. Alter, R. H. Purcell, *Virchows Arch. A Pathol. Anat. Histol.* **387**, 91 (1980).
19. P. Farci *et al.*, *J. Infect. Dis.* **165**, 1006 (1992); M. Shindo, A. M. DiBisceglie, R. Biswas, K. Mihalik, S. M. Feinstone, *ibid.* **166**, 424 (1992).
20. The small amounts of circulating HCV RNA preclude direct determination of 5′-terminal RNA sequences. Therefore, virus derived from transcripts containing the most prevalent 5′ end (5′-GCCA . . . -3′) was distinguished from that derived from transcripts with additional 5′ nucleotides by the presence or absence of the Xho I site at position 514 (Fig. 1). The region containing this marker was amplified by RT-PCR under conditions that ensured that a representative number of independent cDNAs [A. A. Kolykhalov, K. E. Reed, C. M. Rice, in *Hepatitis C Protocols*, J. Y. N. Lau, Ed. (Humana Press, Totowa, NJ), in press] were analyzed (>50 in this case). The resulting products were analyzed for digestion with either Xho I or, as a control, Acc I, an enzyme that should digest this fragment for all input clones. For chimpanzee 1535 (week 3 sample), the fraction of products digested by excess Xho I paralleled the input inoculum: about 20% was digested by Xho I; 80% was resistant to digestion (values were determined by scanning ethidium bromide–stained digestion patterns with an IS-1000 Digital Imaging System, Alpha Innotech Corp.). Complete digestion was observed for Acc I. In the week 4 sample analyzed for chimpanzee 1536, 45% was digested by Xho I; 55% was resistant to digestion. Again, complete digestion was observed for Acc I. Thus, in chimpanzee 1536 an advantage was observed for transcripts without additional 5′ bases (5′-GCCA . . . -3′).
21. Transcripts containing 75-base or 133-base poly(U/UC) tracts were distinguished by the silent marker at nt 8054 in the NS5B coding region (Fig. 1). The region between nt 7955 and 8088 was amplified by RT-PCR, with enough starting material to ensure amplification of >100 independent cDNA molecules [A. A. Kolykhalov, K. E. Reed, C. M. Rice, in *Hepatitis C Protocols*, J. Y. N. Lau, Ed. (Humana Press, Totowa, NJ, in press)], and molecularly cloned. Sequences of 10 and 9 independent clones were determined for chimpanzee 1535 (week 3) and chimpanzee 1536 (week 4), respectively. It was found that 90% (chimpanzee 1535) and 67% (chimpanzee 1536) of the clones contained the G at nt 8054, indicative of the 133-base poly(U/UC) tract. Thus, the 133-base tract appears to be preferred, although we cannot rule out the possibility that this preference was because of a deleterious effect of the marker mutation on the transcripts with the 75-base tract.
22. S. Falkow, *Rev. Infect. Dis.* **10** (Suppl. 2), S274 (1988).
23. A. Grakoui, C. Wychowski, C. Lin, S. M. Feinstone, C. M. Rice, *J. Virol.* **67**, 1385 (1993).
24. We thank C. Read for expert technical assistance, S. Emerson for positive control hepatitis A virus cDNA clones, R. Purcell for generously making available his primate facilities, M. Shapiro for collection and analysis of chimpanzee samples, and A. DiBisceglie for bDNA analyses. We are also grateful to A. Grakoui, M. Heise, and J. A. Lemm for their participation in the early phases of this work and to S. Amberg, D. Goldberg, S. Hultgren, B. Lindenbach, M. MacDonald, J. Majors, and K. Reed for helpful discussion and comments on the manuscript. This work was supported in part by grants from the Public Health Service to C.M.R. (CA57973 and AI40034).

16 April 1997; accepted 19 June 1997

Mitosis in Living Budding Yeast: Anaphase A But No Metaphase Plate

Aaron F. Straight,* Wallace F. Marshall, John W. Sedat, Andrew W. Murray

Chromosome movements and spindle dynamics were visualized in living cells of the budding yeast *Saccharomyces cerevisiae*. Individual chromosomal loci were detected by expression of a protein fusion between green fluorescent protein (GFP) and the Lac repressor, which bound to an array of Lac operator binding sites integrated into the chromosome. Spindle microtubules were detected by expression of a protein fusion between GFP and Tub1, the major alpha tubulin. Spindle elongation and chromosome separation exhibited biphasic kinetics, and centromeres separated before telomeres. Budding yeast did not exhibit a conventional metaphase chromosome alignment but did show anaphase A, movement of the chromosomes to the poles.

The reproduction of eukaryotic cells depends on the ability of the mitotic spindle to segregate the replicated chromosomes into two identical sets. As cells enter mitosis they organize microtubules into a bipolar spindle. In most eukaryotes the kinetochore, a specialized region of the chromosome, binds microtubules, and in higher eukaryotes the condensed chromosomes move to a position equidistant from the spindle poles called the metaphase plate. Once all sister chromatids are properly aligned in metaphase, the linkage between the sister chromatids is dissolved, causing two changes that segregate the sisters from each other: Chromosomes move toward the spindle pole (anaphase A), and elongation of the spindle separates the spindle poles (anaphase B).

Knowledge of mitosis comes from three sources: microscopic observation and manipulation of animal and plant cells (*1*), studies in cell cycle extracts (*2*), and genetic analysis, especially in budding and fission yeast (*3*). To integrate the findings of these different approaches, we need to know if the basic features of mitosis are conserved among eukaryotes. Although the budding yeast *Saccharomyces cerevisiae* is an excellent organism for genetic analysis, its mitotic spindle is small and difficult to see in living cells. Individual mitotic yeast chromosomes are not visible by conventional light or electron microscopy and can only be seen by in situ hybridization to fixed cells (*4*, *5*). We have simultaneously visualized the mitotic spindle and individual chromosomes in living yeast cells. These studies show that (i) budding yeast chromosomes do not align on a metaphase plate, (ii) spindle elongation and chromosome separation exhibit biphasic kinetics, (iii) yeast exhibit anaphase A chromosome-to-pole movement, (iv) chromosomes are under poleward force as they separate, and (v) centromeres separate before telomeres.

We used green fluorescent protein (GFP) (*6*) to follow chromosome and spindle movements in living yeast cells by fluorescence microscopy. We visualized the spindle with a protein fusion between GFP and the major alpha tubulin (Tub1) (*7*). Specific loci were marked by binding of a protein fusion between GFP and the Lac repressor (GFP-LacI) to an integrated array of the Lac operator (LacO) (*8*, *9*). We observed synchronized cells passing through mitosis, taking vertical stacks of images every 26 s and subjecting them to iterative deconvolution (*10*, *11*). The top panel of Fig. 1A shows a series of optical sections after deconvolution projected as a stereo pair to reveal the structure of the entire spindle and the staining of the centromeres

A. F. Straight and A. W. Murray, Department of Physiology, Box 0444, School of Medicine, University of California at San Francisco, San Francisco, CA 94143–0444, USA.
W. F. Marshall and J. W. Sedat, Department of Biochemistry, Box 0448, School of Medicine, University of California at San Francisco, San Francisco, CA 94143–0448, USA.
*To whom correspondence should be addressed.

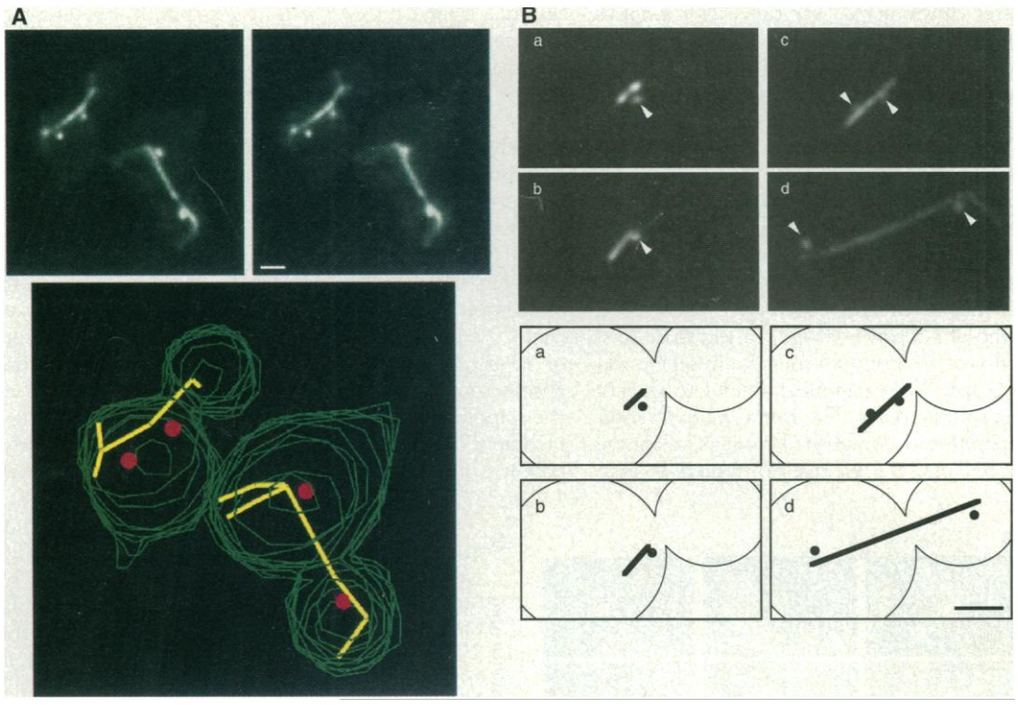

Fig. 1. Visualization of microtubules and chromosomes during mitosis. Images are 2D projections of 3D data sets. Spindle microtubule staining is the bright bar joining the chromosomal staining. (**A**) (Top) Stereo projection of yeast cells during anaphase. Bar, 2 μm. (Bottom) A 3D model of the top panel constructed by tracing the fluorescence intensity in the 3D data. (**B**) (Top) Images from a single cell passing through mitosis (arrowheads mark chromosomal staining). (Bottom) Cartoon of centromeres, spindle, and cell outline. Bar, 2 μm. (a) Early mitosis. A short, bipolar spindle has formed. (b) Onset of anaphase with sister chromatids at one spindle pole. (c) Early anaphase. Sister chromatids have separated and the spindle is elongating. (d) Late anaphase. Chromosomes are distantly separated and spindle has elongated into the daughter cell (*10*).

in three dimensions, and the bottom panel shows a three-dimensional (3D) model of the same cells. Although the chromosomal LacO array and microtubules are both marked with GFP, the two structures are easily distinguished: The LacO array is a spherically symmetrical dot, whereas the spindle is a straight, rod-shaped structure that stains more intensely at its two ends. Although subsequent images are 2D projections of the 3D data, all distances are true distances between objects in 3D space.

Figure 1B shows mitosis in a living yeast cell. Even in the shortest spindles, the GFP-tagged centromeres were close to the spindle's long axis (Fig. 1B). The centromeric staining was not restricted to the central region of the spindle and was often found near one of the spindle poles. Once anaphase began, sister chromatids moved rapidly toward opposite spindle poles along the spindle axis. Finally, spindle elongation distributed one sister chromatid to the mother cell and its partner to the daughter cell.

In animal and plant cells, once the two kinetochores of a pair of sister chromatids have attached to opposite spindle poles, the chromatid pair moves to a point equidistant from the two poles (*12*, *13*). This congression is thought to be achieved by a balance between opposing forces on chromosomes: a poleward force applied at the kinetochore, a polar ejection force or the "polar wind" acting along the length of the chromosome, and forces acting on the attached sister kinetochore (*12*). We examined yeast cells to see if congression occurred in these very small spindles, which appear to lack the nonkinetochore microtubules that have been postulated to be responsible for the polar wind (*14*). We observed multiple cells (6 out of 14) in which the centromeric staining moved back and forth along the long axis of the spindle (Fig. 2, A and B). The oscillations spanned the length of the spindle (1.5 to 2.0 μm) and continued until anaphase began (t = 0 s). Animal and plant chromosomes also oscillate along the spindle axis, and the absolute magnitude of the oscillations is similar to that seen in yeast. Unlike yeast spindles, however, the relative amplitude of these movements is much less than the length of the spindle so that the oscillations do not bring chromosomes near the poles. Centromere oscillation along the spindle axis implies that either kinetochores detach from and reattach to spindle microtubules or that microtubules lengthen and shorten while attached to the kinetochore, as occurs in higher eukaryotes (*15*). Detachment and reattachment of kinetochores to microtubules seems unlikely because yeast appear to have a single microtubule per kinetochore (*16*, *17*) and unattached kinetochores would activate the spindle assembly checkpoint (*18*). Thus, chromosome oscillations suggest that an individual microtubule can polymerize and depolymerize while maintaining attachment to a yeast kinetochore.

Yeast cells often initiate anaphase when the centromeres are closer to one pole than the other. Figure 2A shows a chromosomal spot abutting one spindle pole immediately before anaphase chromosome separation. Ten out of 17 cells (59%) initiated anaphase when the centromere was within the terminal 25% of the spindle, and 7 (41%) did so when the centromere was between 25 and 75% of the distance along the spindle. This observation suggests that budding yeast lack a conventional metaphase plate and that chromosomal alignment on a metaphase plate is not required for anaphase chromosome separation in *S. cerevisiae*. This result is consistent with fixed cell studies that show that chromosomes are distributed along the length of the metaphase spindle and that presumptive kinetochore microtubules do not exhibit a metaphase arrangement (*4*, *17*, *19*, *20*). Although the chromosomes often separated when the sister chromatid pair was near one of the spindle poles, both sister chromatids never moved to the same pole. Thus, the sister kinetochores on all the observed chromosomes were attached to opposite spindle poles before the onset of anaphase, satisfying the cell cycle checkpoint that senses kinetochore attachment to the spindle microtubules (*18*, *21*).

Successive images of anaphase in a single cell are shown in Fig. 3A. We measured all the pairwise distances between the spindle poles and the kinetochores of the sister chromatids as cells proceeded through mitosis and aligned the records from various cells by defining t = 0 as the moment of sister chromatid separation. Figure 3B shows the average distance between the spindle poles and the distance between the

sister centromeres over time. The kinetics of anaphase were highly reproducible from cell to cell. The bipolar mitotic spindle was between 1.5 and 2.0 μm in length for many minutes before the initiation of anaphase. Two minutes before sister chromatid separation, the rate of spindle elongation gradually increased to 0.54 μm/min, and the spindle was between 2.5 and 3.0 μm long when chromosome separation began (Fig. 3B). In contrast to this smooth increase, the separation of the centromeres showed a jump of 1.8 μm (average) in less than 26 s, followed by a smooth increase in separation at a rate (0.64 μm/min) similar to that of the spindle poles. The initial jump in sister separation accomplished most of anaphase A, reducing the average centromere-to-pole distance from 1.5 to 0.7 μm in less than a minute. The abrupt separation of the sister chromatids suggests that either their linkage to the poles is under poleward force before sister separation or that there is some repulsive force between the chromosomes that propels them apart once the linkage between them is dissolved. The rapid phase of elongation and separation continued until the spindle length increased to 5.0 to 6.0 μm (Fig. 3B). At this point both spindle elongation and sister separation slowed to about 0.2 μm/min, reaching a final extent of 10 to 11 μm (Fig. 3B). However, the chromosomes continued to separate with the spindle, indicating that microtubule attachment of the chromosome to the spindle pole was still intact. These results are consistent with rates of spindle elongation measured by differential interference contrast microscopy in another wild-type strain (*22*). In most of the cells the rapid phases of both sister separation and spindle elongation occurred through the bud neck. In 2 out of 17 mitoses, however, the initial phase of separation occurred entirely within the mother cell and was followed by reorientation of the spindle and its slow elongation through the bud neck.

The unusual property that chromosomes can separate when they are much nearer one spindle pole than the other allowed us to investigate anaphase A in yeast. Figure 3A shows images from a cell that started anaphase when chromosomes were close to one spindle pole body. At $t = 0$ the chromatid pair was still joined but was very close to one spindle pole body (Fig. 3A). At the next time point ($t = 26$ s) the chromatid pair had clearly separated, and one chromatid had moved toward the more distant spindle pole. After this chromosome-to-pole movement, the spindle elongated and separated the sister chromatids into the mother and daughter cells (Fig. 3A). Figure 3C shows the distance between the sister chromatids, the distance between the chromatid that began anaphase near its spindle pole and its spindle pole, and the distance between the sister chromatid that began anaphase far from its spindle pole and its spindle pole, with respect to time. Once sister chromatid separation began, the chromatid that was far away from its spindle pole moved rapidly toward that pole at a rate of at least 1.33 μm/min. The chro-

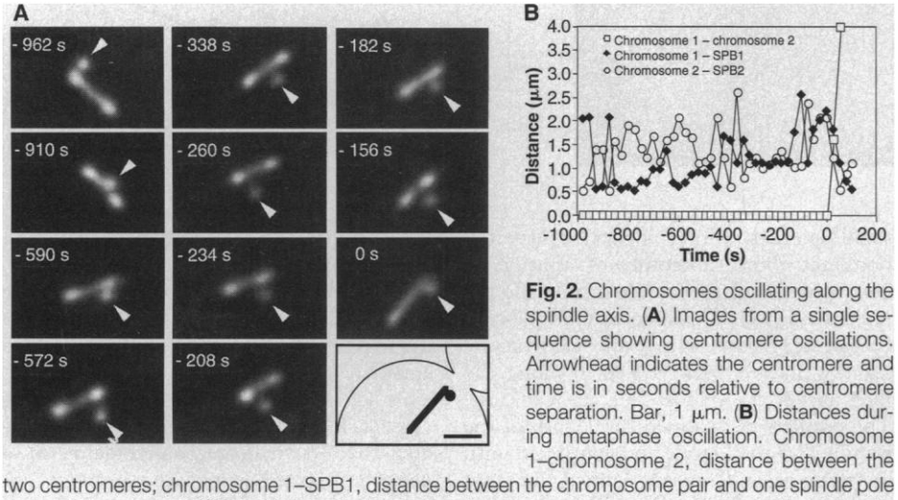

Fig. 2. Chromosomes oscillating along the spindle axis. (**A**) Images from a single sequence showing centromere oscillations. Arrowhead indicates the centromere and time is in seconds relative to centromere separation. Bar, 1 μm. (**B**) Distances during metaphase oscillation. Chromosome 1–chromosome 2, distance between the two centromeres; chromosome 1–SPB1, distance between the chromosome pair and one spindle pole body; chromosome 2–SPB2, distance between the chromosome pair and the other spindle pole body.

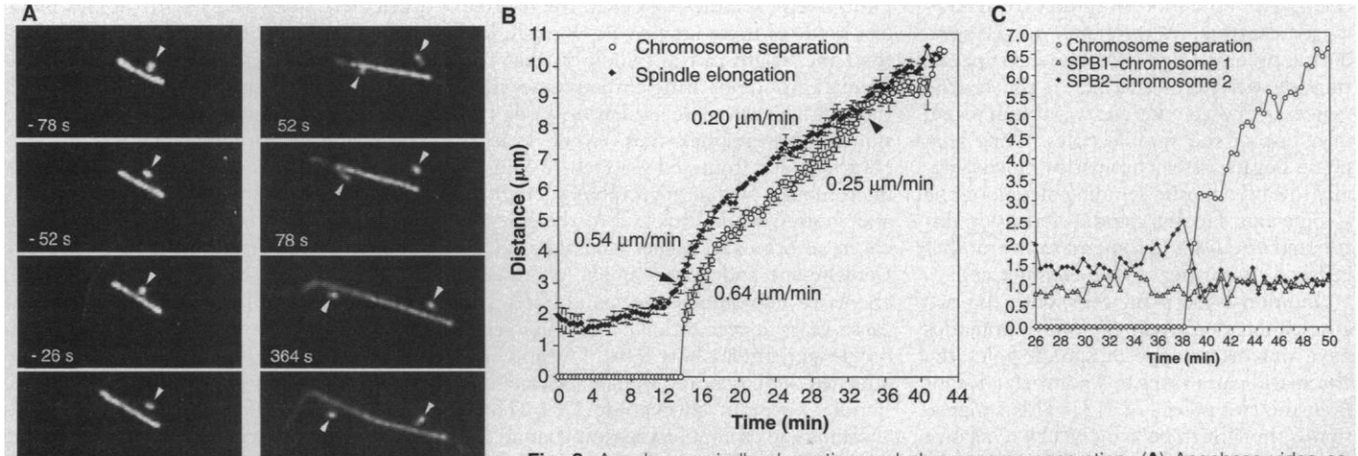

Fig. 3. Anaphase spindle elongation and chromosome separation. (**A**) Anaphase video sequence. Arrowheads mark centromeres, time is in seconds relative to sister chromatid separation, cartoon shows cell outline. Bar, 2 μm. (**B**) Kinetics of anaphase. Distances were measured between spindle pole bodies and chromosomal spots (*25*) in six data sets aligned by defining the time of chromosome separation as $t = 0$ (arrow on the pole separation trace). Arrowhead, time when chromosomes reached the same separation as the spindle poles. Rates of movement were derived by linear regression, and all correlation coefficients exceed 0.99. (**C**) Observation of anaphase A chromosome movement. Chromosome-to-pole distance was calculated for cells that exhibit biased anaphase initiation ($n = 3$).

matid that was near its spindle pole moved little if at all.

Our analysis of chromosome movement to the spindle pole indicates that, in yeast, proximity of the sister chromatid pair to the spindle pole is not the activating signal for the mitotic checkpoint (*23*). Loss of tension on a kinetochore activates the spindle checkpoint in insect spermatocytes (*24*). Our observation that chromatid pairs close to one spindle pole appear to satisfy the spindle assembly checkpoint suggests that either there is sufficient tension on both kinetochores to prevent the activation of the checkpoint, or the yeast checkpoint monitors a parameter other than tension. Yeast are responsive to excess kinetochores (*21*), and in higher eukaryotic cells unattached kinetochores activate the spindle assembly checkpoint (*18*), but it is still unclear how yeast cells sense defects at the kinetochore.

To investigate the role of microtubule-dependent forces in chromosome separation, we observed mitosis in cells that lacked a spindle but still progressed through mitosis. The spindle assembly checkpoint mutant *mad1* does not sense spindle depolymerization and proceeds through mitosis even though it cannot accurately segregate its sister chromatids. We constructed a *mad1* yeast strain that contained the GFP-LacI tag at the centromere of chromosome III and followed mitosis in the presence of nocodazole (15 μg/ml, a concentration that depolymerizes all microtubules). The first detectable instance of sister centromere separation occurred at t = 26 s (Fig. 4A), but in the absence of a spindle there was no efficient segregation of the chromosomes. Instead, the GFP-marked LacO arrays repeatedly separated into two separate dots and then approached each other so closely that they could no longer be resolved and appeared as a single dot. Sister chromatid separation in *mad1* mutants in the presence of nocodazole was compared to that in wild-type cells in the absence of nocodazole (Fig. 4B). In *mad1* cells, sister chromatids never separated more than 1.5 to 2.0 μm from each other, whereas chromatids in wild-type cells separated 2 to 2.5 μm within 52 s after disjunction (Fig. 4B), demonstrating that chromosome segregation requires the microtubule-dependent forces exerted by an intact spindle.

During anaphase in higher eukaryotes, chromosomes move toward the poles with their centromeres leading and their telomeres lagging behind. To visualize the centromere and telomere of the same chromosome in yeast, we integrated the LacO array both at the centromere and near the telomere of the long arm of chromosome IV, 1000 kb apart. A fortuitous recombination event reduced the size of the telomeric LacO array, allowing us to differentiate the weaker fluorescence of the telomeric array from the centromeric one. Before separation, the centromere and telomere stained

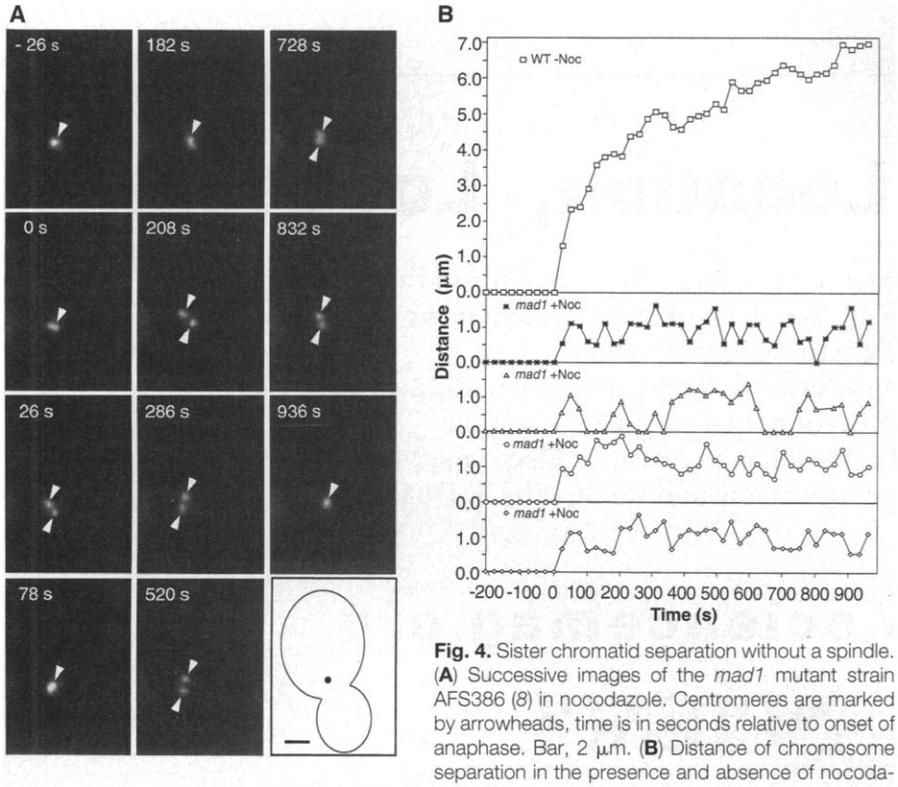

Fig. 4. Sister chromatid separation without a spindle. (**A**) Successive images of the *mad1* mutant strain AFS386 (*8*) in nocodazole. Centromeres are marked by arrowheads, time is in seconds relative to onset of anaphase. Bar, 2 μm. (**B**) Distance of chromosome separation in the presence and absence of nocodazole. WT −Noc, chromatid separation in the presence of a spindle; *mad1* +Noc, distances from four separate video sequences in the presence of nocodazole.

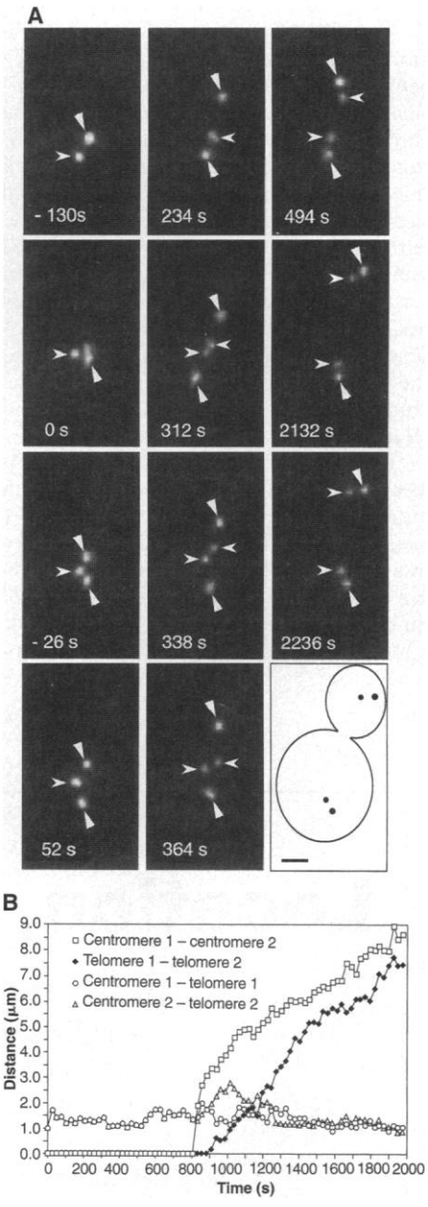

Fig. 5. Centromere and telomere separation. (**A**) Successive images showing the separation of the centromeres and telomeres of chromosome IV in yeast strain AFS412 (*26*). Arrowheads, centromeres; barbed arrowheads, telomeres. Bar, 2 μm. Time is in seconds relative to centromere separation. (**B**) Distance between centromeres and telomeres. Shown is the average of five video sequences of centromere and telomere separation. The centromere and telomere that remained in the mother cell are labeled centromere 1 and telomere 1, and the centromere and telomere that were distributed to the daughter cell are labeled centromere 2 and telomere 2.

as two discernible spots (Fig. 5A), and in all cells the centromeres separated 1 to 3 min before the telomeres. The kinetics of centromere and telomere separation were measured as an average of five video sequences (Fig. 5B). The centromeres of chromosome IV separated with kinetics nearly identical to those of the centromeres of chromosome III (Fig. 5B). The telomeres lagged in the kinetics of their separation. The distance between centromere 2 and telomere 2 increased then decreased, suggesting that the chromatin strand was stretched as the centromere was dragged into the daughter cell (Fig. 5B) and that this stretch was relieved as the telomere approached the centromere. Although the centromeres separated smoothly, the rate of telomere separation varied during anaphase. This difference may result from the active pulling on the centromere region by the spindle as opposed to the elastic stretching and recoiling of the chromatin that links the centromere and telomere.

The relative importance of various mechanisms of chromosome movement in mitosis has not been established and may vary between cell types. The ability to see individual chromosome movements in living yeast should allow detailed analysis of the phenotypes of mutations in microtubule motors and components of the mitotic apparatus and contribute to understanding of the dynamics and mechanism of mitosis.

REFERENCES AND NOTES

1. R. B. Nicklas, *Science* **275**, 632 (1997).
2. A. W. Murray, *Methods Cell Biol.* **36**, 573 (1991).
3. B. D. Page and M. Snyder, *Annu. Rev. Microbiol.* **47**, 231 (1993).
4. V. Guacci, E. Hogan, D. Koshland, *J. Cell Biol.* **125**, 517 (1994).
5. H. Scherthan, J. Loidl, T. Schuster, D. Schweizer, *Chromosoma* **101**, 590 (1992).
6. D. C. Prasher, *Trends Genet.* **11**, 320 (1995).
7. The GFP-Tub1 fusion under the control of the HIS3 promoter was constructed by ligating the entire genomic TUB1 locus with Bam HI and Not I linkers into pAFS78 (*8*). The resultant GFP-Tub1 fusion was cloned into the Kpn I to Xho I sites of pRS306 to yield pAFS91 and integrated at the URA3 locus after Stu I digestion. The GFP-tubulin fusion was functional because it rescues a normally lethal TUB1 deletion. Strain AFS403 was constructed by transforming strain AFS173 (*8*) with Stu I–digested pAFS91.
8. A. F. Straight, C. C. Robinett, A. S. Belmont, A. W. Murray, *Curr. Biol.* **6**, 1599 (1996).
9. C. C. Robinett *et al.*, *J. Cell Biol.* **135**, 1685 (1996).
10. AFS403 is a *MAT***a** strain carrying the GFP-Tub1 and GFP-LacI fusions as well as a Lac operator array located 23 kb from the centromere of chromosome III. Cells were synchronized in G_1 by treatment with α-factor (10 μg/ml) for 3 hours, released from this arrest, induced to express the GFP-Tub1 and GFP-LacI fusions for 30 min (*8*), and mounted in histidine-free medium. Every 26 s, 12 optical sections (100-ms exposure time) were collected (vertical separation, 0.5 μm) by wide-field deconvolution 3D microscopy (*11*) with a 60× 1.4 numerical aperture lens.
11. D. A. Agard, Y. Hiraoka, P. Shaw, J. W. Sedat, *Methods Cell Biol.* **30**, 353 (1989).
12. R. V. Skibbens, V. P. Skeen, E. D. Salmon, *J. Cell Biol.* **122**, 859 (1993).
13. A. S. Bajer and J. Molè-Bajer, *ibid.* **102**, 263 (1986).
14. C. L. Rieder and E. D. Salmon, *ibid.* **124**, 223 (1994).
15. T. J. Mitchison, *Annu. Rev. Cell Biol.* **4**, 527 (1988).
16. J. B. Peterson and H. Ris, *J. Cell Sci.* **22**, 219 (1976).
17. M. Winey *et al.*, *J. Cell Biol.* **129**, 1601 (1995).
18. C. L. Rieder, R. W. Cole, A. Khodjakov, G. Sluder, *ibid.* **130**, 941 (1995).
19. P. Y. Goh and J. V. Kilmartin, *ibid.* **121**, 503 (1993).
20. V. Guacci, E. Hogan, D. Koshland, *Mol. Biol. Cell.* **8**, (1997).
21. W. A. E. Wells and A. W. Murray, *J. Cell Biol.* **133**, 75 (1996).
22. E. Yeh, R. V. Skibbens, J. W. Cheng, E. D. Salmon, K. Bloom, *ibid.* **130**, 687 (1995).
23. R. B. Nicklas and P. Arana, *J. Cell Sci.* **102**, 681 (1992).
24. R. B. Nicklas, S. C. Ward, G. J. Gorbsky, *J. Cell Biol.* **130**, 929 (1995).
25. H. Chen, D. D. Hughes, T. A. Chan, J. W. Sedat, D. A. Agard, *J. Struct. Biol.* **116**, 56 (1996).
26. Strain AFS412 was constructed by integrating pAFS52 (*8*) at TRP1 near the centromere of chromosome IV and then integrating pAFS114 near the telomere of chromosome IV. Plasmid pAFS114 contains a Kpn I–Sac I fragment of chromosome IV spanning nucleotides 1,436,502 to 1,438,325 in pAFS59 (*8*) and was integrated into chromosome IV after digestion with Bsa BI.

27. We thank members of the Murray laboratory; D. O. Morgan and A. Farrell for critical review of the manuscript; A. Desai, T. J. Mitchison, and H. Funabiki for insightful comments and discussion; and J. Fung and S. Parmelee for assistance during data analysis. Supported by grants from NIH and the Packard Foundation.

13 March 1997; accepted 18 June 1997